Acta Crystallographica Section F
Structural Biology and Crystallization Communications
ISSN 1744-3091

Crystallization and X-ray structure analysis of a thermostable penicillin G acylase from *Alcaligenes faecalis*

Nishant Kumar Varshney,[a] R. Suresh Kumar,[a] Zoya Ignatova,[b] Asmita Prabhune,[a] Archana Pundle,[a] Eleanor Dodson[c] and C. G. Suresh[a]*

[a]Division of Biochemical Sciences, National Chemical Laboratory, Pune 411 008, India, [b]Department of Biochemistry, Institute of Biochemistry and Biology, University of Potsdam, 14476 Potsdam, Germany, and [c]York Structural Biology Laboratory, University of York, York YO10 5DD, England

Correspondence e-mail: cg.suresh@ncl.res.in

Received 26 September 2011
Accepted 14 December 2011

PDB References: penicillin G acylase, orthorhombic, 3k3w; tetragonal, 3ml0.

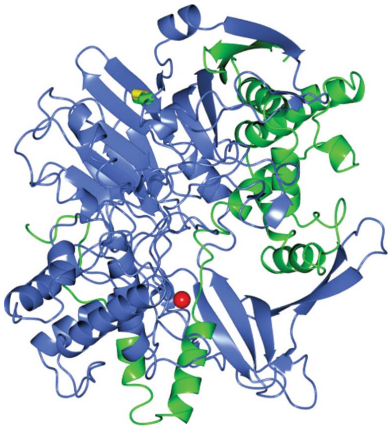

The enzyme penicillin G acylase (EC 3.5.1.11) catalyzes amide-bond cleavage in benzylpenicillin (penicillin G) to yield 6-aminopenicillanic acid, an intermediate chemical used in the production of semisynthetic penicillins. A thermostable penicillin G acylase from *Alcaligenes faecalis* (*Af*PGA) has been crystallized using the hanging-drop vapour-diffusion method in two different space groups: $C222_1$, with unit-cell parameters $a = 72.9$, $b = 86.0$, $c = 260.2$ Å, and $P4_12_12$, with unit-cell parameters $a = b = 85.6$, $c = 298.8$ Å. Data were collected at 293 K and the structure was determined using the molecular-replacement method. Like other penicillin acylases, *Af*PGA belongs to the N-terminal nucleophilic hydrolase superfamily, has undergone post-translational processing and has a serine as the N-terminal residue of the β-chain. A disulfide bridge has been identified in the structure that was not found in the other two known penicillin G acylase structures. The presence of the disulfide bridge is perceived to be one factor that confers higher stability to this enzyme.

1. Introduction

Penicillins are the most widely used β-lactam antibiotics, with a share of about 20% of the estimated worldwide antibiotic market, owing to their inhibitory action towards bacterial cell-wall synthesis. In general, they possess broad-spectrum antibacterial activity, low toxicity and outstanding efficacy against various bacterial strains. However, the excessive use of these antibacterials has led to the development of several resistant pathogens. One effective method of overcoming resistance is by the use of newer semisynthetic antibiotics (Parmar *et al.*, 2000).

Most of the new semisynthetic penicillins are industrially produced from 6-aminopenicillanic acid (6-APA) and 7-amino-3-deacetoxy-cephalosporanic acid (7-ADCA), which in turn are mainly produced by enzymatic or chemical deacylation of the natural penicillins. Relative to chemical synthesis, enzymatic synthesis is environmentally friendly. Penicillin acylase or penicillin amidohydrolase (EC 3.5.1.11) is the enzyme that is most often employed for large-scale production of 6-APA or 7-ADCA. In addition, penicillin acylases are useful as biocatalysts in many potentially valuable reactions, such as the protection of amino and hydroxyl groups in peptide synthesis as well as the resolution of racemic mixtures of chiral compounds (Arroyo *et al.*, 2003).

Penicillin acylases belong to the N-terminal nucleophile (Ntn) hydrolase superfamily of enzymes (Brannigan *et al.*, 1995). The PGA enzymes, like other members of the family, are produced as precursor molecules (pre-pro-proteins) and undergo a post-translational processing step that leads to an autocatalytically activated form (Kasche *et al.*, 1999). This process contains two essential steps: translocation of the precursor to the periplasmic membrane and processing of the precursor by an autocatalytic intramolecular peptide-bond cleavage.

The rate-limiting step in the production of active enzyme is the intramolecular autoproteolytic processing of the precursor molecule, resulting in the removal of a linker peptide. This processing leads to the formation of a heterodimeric enzyme with two polypeptide chains, α and β, and a free N-terminal serine in the β-chain which is essential for activity of the enzyme (Duggleby *et al.*, 1995). Somewhat surprisingly, this processing is similar to the processing of other

pre-pro-proteins, including higher eukaryotic peptide pre-pro-hormones such as prothrombin and meizothrombin (Petrovan *et al.*, 1998), viral proteins such as the coat protein of flock house virus belonging to the nodavirus family (Zlotnick *et al.*, 1994; Wu *et al.*, 1998), the Hedgehog protein (Lee *et al.*, 1994) and enzymes such as glycosylasparaginase (Guan *et al.*, 1996; Wang & Guo, 2010). Caspases, which like penicillin amidase are important regulators of apoptosis, are activated by the removal of a linker peptide in the proenzyme (Stennicke & Salvesen, 1998). This processing phenomenon is not common in proteins from prokaryotic systems (Sizmann *et al.*, 1990).

The enzymes of the Ntn hydrolase superfamily display a remarkable variety of hydrolytic activities (Suresh *et al.*, 1999; McVey *et al.*, 2001). The typical fold of the Ntn hydrolase superfamily consists of a four-layered catalytically active $\alpha\beta\beta\alpha$ core structure (Oinonen & Rouvinen, 2000). This core is formed by two antiparallel β-sheets packed against each other and these β-sheets are sandwiched by a layer of α-helices on either side.

The penicillin acylases are grouped into three classes according to their substrate specificity: (i) penicillin G acylases (PGAs), which preferentially hydrolyze penicillin G (benzylpenicillin); (ii) penicillin V acylases (PVAs), which preferentially hydrolyze penicillin V (phenoxymethylpenicillin); and (iii) ampicillin acylases, which specifically hydrolyze ampicillin (Deshpande *et al.*, 1994). Both PGA and PVA are currently being used for the industrial production of 6-APA.

Crystal structures of PGAs from two sources have been reported: those from *Escherichia coli* (Duggleby *et al.*, 1995) and *Providencia rettgeri* (McDonough *et al.*, 1999). In this communication, we describe the crystallization and X-ray structure determination of penicillin G acylase from *Alcaligenes faecalis* (*Af*PGA). Although *Af*PGA shares many common features with the other known PGAs, it has a clear industrial advantage over other penicillin acylases in β-lactam conversion because of its higher thermostability and synthetic efficiency in enantioselective synthesis. This makes *Af*PGA a more attractive biocatalyst for both hydrolysis and synthetic conversions. The *E. coli* enzyme is reported to irreversibly lose more than 50% of its activity on incubation at 323 K for 20 min, whereas *Af*PGA is not affected by the same treatment. A putative disulfide bond in *Af*PGA between two cysteine residues in the sequence has been proposed to confer this additional stability to the enzyme (Verhaert *et al.*, 1997). More detailed structural study is expected to provide specific information on the factors that influence the thermostability of this enzyme.

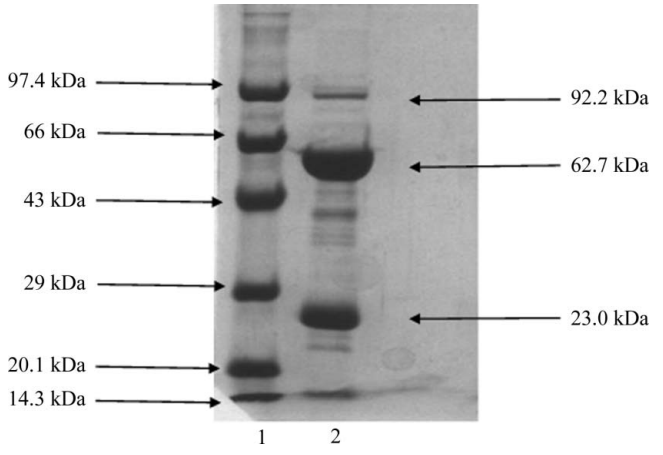

Figure 1
An SDS–PAGE gel showing the presence of the α-subunit (23 kDa) and β-subunit (62.7 kDa) of *Af*PGA. Lane 1, molecular-weight markers (labelled in kDa); lane 2, *Af*PGA.

Our crystallization efforts yielded two crystal forms of *Af*PGA; the growth of a particular crystal form depended on the amount of detergent that was present in the crystallization solution. An analysis of the three-dimensional structure of *Af*PGA pertaining to its characteristic molecular and structural features would improve our general understanding of the nature of the thermostability of this class of enzymes.

2. Materials and methods

2.1. Protein preparation

*Af*PGA shares 49% DNA-sequence identity and 39% protein-sequence identity with the more elaborately studied *E. coli* penicillin acylase (*Ec*PGA). *Af*PGA is expressed as a 92 kDa precursor polypeptide consisting of a signal peptide of length 26 amino acids and α- and β-subunits consisting of 202 and 551 amino acids, respectively, separated by an endopeptide consisting of 37 amino acids which is excised and removed during post-translational processing. Details of the cloning, isolation and purification of *Af*PGA have been described by Ignatova *et al.* (1998) and Kasche *et al.* (2003). Briefly, *A. faecalis* ATCC 1908 chromosomal DNA was used as a template to amplify the PGA gene and cloned in pMMB207 plasmid, yielding pPAAF plasmid (Kasche *et al.*, 2003). *E. coli* BL21 (DE3) strain was used as an expression host. The recombinant strain was grown at 303 K in minimal M9 medium containing 2.5 g l^{-1} glucose. The expression of the *Af*PGA protein was induced with isopropyl β-D-1-thiogalactopyranoside (IPTG; 0.5 m*M*). The cells were harvested 6 h after induction and fractionated into periplasmic and cytoplasmic fractions; *Af*PGA was isolated by single-step anion-exchange chromatography as described in Ignatova *et al.* (1998). The *Af*PGA sample was checked for purity using SDS–PAGE. Two bands corresponding to the α-subunit (23 kDa) and β-subunit (62.7 kDa) were confirmed. In addition, a minor band corresponding to the precursor protein (92.2 kDa) was also present, presumably owing to a minute quantity of misfolded unprocessed PGA being carried over from the sample preparation (Fig. 1).

The protein was prepared for crystallization trials by dialyzing the sample overnight against 10 m*M* potassium phosphate buffer solution pH 7.5 with two changes. The buffer volume was 100 times the volume of the protein solution. Finally, the sample solution was concentrated to about 15 mg ml^{-1} protein using a Centricon concentrator (Millipore) at 5000*g* and stored at 253 K. The concentration of the protein in the sample was estimated by the method of Lowry *et al.* (1951) using BSA as standard.

2.2. Crystallization

All crystallization experiments were carried out at 303 K using the hanging-drop vapour-diffusion method. Commercial sparse-matrix screens such as Crystal Screen and Crystal Screen 2 (Hampton Research, USA) and Clear Strategy Screens I and II (Molecular Dimensions Ltd, UK) were used for initial trials. The protein samples were thawed immediately prior to setting up crystallization and were centrifuged for 5 min at 10 000 rev min^{-1} and 278 K to free the sample of particulate matter. In all experiments, 1 µl protein solution was mixed with 1 µl screen solution and was equilibrated over a reservoir containing 0.5 ml screen solution in 24-well plates (Axygen Biosciences, USA). Trials using the abovementioned commercial screening solutions did not yield crystals.

Crystallization trials were then conducted using locally prepared solutions of precipitants such as polyethylene glycol (PEG) of various sizes in the concentration range 5–25%(*w*/*v*), salts such as ammonium

sulfate (20–70% saturation), organic precipitants such as MPD [20–50%(*v*/*v*)] and various buffers such as citrate (pH 3–5), citrate–phosphate (pH 5–6), phosphate (pH 6–7) and Tris–HCl (pH 7–9). Crystallization trials were conducted by independently varying the precipitant concentration and the pH of the buffer. The addition of various additives such as detergents and alcohols in small quantities (10–100 µl) to the well solution was also tried. During these trials, crystals surrounded by heavy precipitate appeared using a solution of PEG 8000 mixed with buffer near neutral pH. To improve the crystal quality, fine screening of the precipitant concentration and buffer pH was carried out. Finally, the addition of detergent at varying concentrations helped to improve the crystal quality.

2.3. Data collection and processing

Diffraction data were collected at room temperature (293 K) from a crystal mounted inside a sealed thin glass capillary of 1.5 mm in diameter (Hampton Research). Data were recorded on an R-AXIS IV^{++} image plate using Cu $K\alpha$ radiation generated by a Rigaku X-ray generator. The crystal-to-detector distance was kept at 260 mm for orthorhombic crystals and 300 mm for tetragonal crystals. Successive frames were collected using a crystal oscillation of 0.5°. The diffraction data were processed and scaled using *DENZO* and *SCALEPACK* from the *HKL*-2000 suite (Otwinowski & Minor, 1997).

2.4. Structure determination and refinement

Reflections in both space groups were phased using the program *Phaser* from the *CCP*4 suite (McCoy *et al.*, 2007; Winn *et al.*, 2011). The known structure of *Ec*PGA was used as a model. The correct solution was decided based on estimated values of the *Z* score and *R* factor. Initial model building was performed using *Buccaneer* (Cowtan, 2006), which built 660 residues in the $C222_1$ crystal and 740 residues in the $P4_12_12$ crystal. Manual building and correction of the model based on observed electron density in *Coot* (Emsley & Cowtan, 2004) and refinement using *REFMAC*5 (Murshudov *et al.*, 2011) from the pre-release *CCP*4 v.6.1 further reduced the *R* factors.

3. Results

3.1. Experimental results

Reproducible diffraction-quality crystals were grown from crystallization solution consisting of 15%(*w*/*v*) PEG 8000, 0.1 *M* Tris–HCl pH 7.5 and 0.5%(*w*/*v*) β-octyl-glucopyranoside solution. The presence of 60 µl β-octyl-glucopyranoside in the well solution led to orthorhombic crystals (Fig. 2*a*), whereas 100 µl β-octyl-glucopyranoside resulted in tetragonal crystals (Fig. 2*b*). Varying the concentration of β-octyl-glucopyranoside resulted in crystals of varying morphology, but these were not better than the two forms analysed. For example, very thin plate-type crystals that were difficult to handle and that diffracted poorly were obtained in the presence of 70 µl 0.5%(*w*/*v*) β-octyl-glucopyranoside solution (data not shown).

The collection of high-resolution data was limited by deterioration of diffraction quality on freezing the crystals under cryoconditions. Trials using a number of cryoprotectants such as PEG 400, glycerol, ethylene glycol, 2-propanol and hexanetriol at concentrations of 20–30% in the crystallization solution, combined with strategies of slow and fast soaking in cryosolution, did not help. Soaking crystals in cryoprotectants invariably resulted in unmanageable mosaicity or in total elimination of diffraction.

The orthorhombic data could be processed in either space group *C*222, with unit-cell parameters a = 72.9, b = 86.0, c = 260.2 Å, or in space group *P*2, with unit-cell parameters a = 56.4, b = 260.2, c = 56.4 Å, β = 99.4°. Since tests for the presence of twinning were negative, the higher symmetry was chosen. These crystals diffracted to 3.3 Å resolution. Tetragonal-type crystals were indexed in space group *P*422, with unit-cell parameters $a = b$ = 85.6, c = 298.8 Å, and diffracted to 3.5 Å resolution. Although diffraction extended slightly beyond these resolutions, the data could not be processed because of asymmetry of the diffraction and a sharp rise in $R_{\rm merge}$. Although several data sets were collected with varying quality, the statistics are summarized in Table 1 for the sets which gave the best $R_{\rm merge}$ for this resolution. Assuming a molecular weight of 86 kDa and one molecule in the asymmetric unit of both crystal forms, the estimated Matthews coefficients $V_{\rm M}$ were 2.37 Å^3 Da^{-1} for the orthorhombic form and 3.18 Å^3 Da^{-1} for the tetragonal form, which correspond to solvent contents of 48 and 61%, respectively. These values were within the normal ranges found in protein crystals (Matthews, 1968).

Table 1
Data-collection and data-processing statistics for the orthorhombic and tetragonal crystal forms of *Af*PGA.

Values in parentheses are for the highest resolution shell.

	Orthorhombic form	Tetragonal form
Detector	R-AXIS IV^{++}	R-AXIS IV^{++}
Wavelength (Å)	1.541	1.541
Space group	$C222_1$	$P4_12_12$
Resolution range (Å)	50–3.30 (3.42–3.30)	20–3.50 (3.56–3.50)
Unit-cell parameters (Å)	a = 72.9, b = 86.0, c = 260.2	$a = b$ = 85.6, c = 298.8
Molecules in asymmetric unit	1	1
Matthews coefficient (Å^3 Da^{-1})	2.37	3.18
Solvent content (%)	48	61
No. of observed reflections	120675	99602
No. of unique reflections	12632	40387
Multiplicity	3.7 (3.3)	2.3 (2.0)
Average $I/\sigma(I)$	8.6 (3.8)	7.4 (3.1)
$R_{\rm merge}$† (%)	11.6 (28.8)	9.9 (23.9)
Completeness (%)	99.6 (97.9)	90.5 (95.4)

† $R_{\rm merge} = \sum_{hkl}\sum_i |I_i(hkl) - \langle I(hkl)\rangle| / \sum_{hkl}\sum_i I_i(hkl)$, where $I_i(hkl)$ is the intensity of the ith observation and $\langle I(hkl)\rangle$ is the mean intensity of the reflections.

3.2. Molecular-replacement solution and structure refinement

Trials for determination of the structure were performed using the molecular-replacement method with the structure of penicillin G acylase from *E. coli* in the processed form at 1.3 Å resolution (PDB entry 1gk9; McVey *et al.*, 2001) as a template. Structure solutions for both space groups were obtained using the program *Phaser* from the *CCP*4 suite. The estimated values of the *Z* score and *R* factor were used as indicators of the choice of the correct solution. In the case of

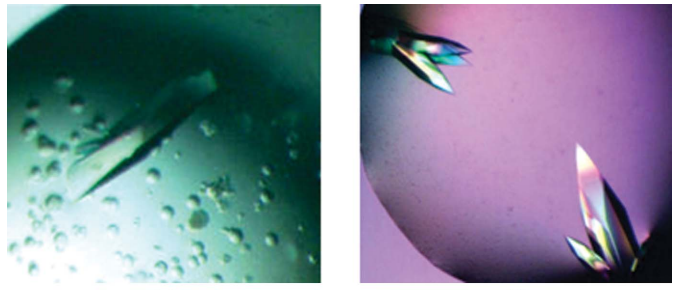

(*a*) (*b*)

Figure 2
Two crystal forms that grew in 15% PEG 8000 and 0.1 *M* Tris–HCl pH 7.5 with different concentrations of β-octyl-glucopyranoside. (*a*) Orthorhombic crystals obtained using 60 µl 0.5%(*w*/*v*) β-octyl-glucopyranoside; (*b*) tetragonal crystals grown using 80–100 µl 0.5%(*w*/*v*) β-octyl-glucopyranoside.

Table 2
Structure-refinement parameters for the orthogonal and tetragonal crystal forms of *Af*PGA.

	Orthorhombic form	Tetragonal form
Resolution range for refinement (Å)	46.82–3.31	20.00–3.49
R_{work}†	0.283	0.269
R_{free}†	0.315	0.283
Ramachandran map analysis‡ (%)		
Residues in most favoured regions	87.4	88.9
Residues in additional allowed regions	12.4	10.1
Residues in generously allowed regions	0.2	0.6

† R_{work} and R_{free} are defined by $R = \sum_{hkl} ||F_{obs}| - |F_{calc}|| / \sum_{hkl} |F_{obs}|$, where *hkl* are the indices of the reflections (reflections used in refinement for R_{work}; 5% reflections not used in refinement for R_{free}). ‡ Ramachandran analysis using *PROCHECK* (Laskowski *et al.*, 1993).

the orthorhombic form, space group $C222_1$ was chosen based on systematic absences and a lower R_{merge} in diffraction data processing. Diffraction data from the orthorhombic crystal form in the resolution range 20–3.3 Å were used in the molecular-replacement search and a unique solution with a correlation coefficient of 44.4% and an R factor of 48.6% was selected.

For the tetragonal form, diffraction data in the resolution range 20–3.5 Å were used. All possible alternative space groups ($P422$, $P42_12$, $P4_122$, $P4_12_12$, $P4_222$, $P4_22_12$, $P4_322$ and $P4_32_12$) were used in calculation of the translation function. The solution that corresponded to the highest Z score, in space group $P4_12_12$, was then subjected to packing-function calculations and showed the permissible number of clashes, which in this case was fixed as zero. The correlation coefficient of the solution was 45.5% and the R factor was 49.1%. The final R/R_{free} after refinement for the orthorhombic and tetragonal forms were 0.27/0.31 and 0.25/0.30, respectively. The refinement parameters are listed in Table 2. The structure factors and coordinates have been deposited in the Protein Data Bank (PDB; http://www.rcsb.org/pdb) under accession codes 3k3w and 3ml0.

3.3. Description of the structure

The α-chains and β-chains of the heterodimer are closely intertwined to form a pyramidal structure (Fig. 3). *PROMOTIF* analysis using *PDBsum* (http://www.ebi.ac.uk/pdbsum/) of the structure in the orthorhombic form showed seven β-sheets and 25 helices. The α-chain consists of two strands and ten helices; their connecting segments form one β-hairpin, two β-bulges, 30 β-turns and two γ-turns. Similarly, the β-chain consists of 26 strands and 15 helices, and the connecting segments form 12 β-hairpins, two β-bulges, 67 β-turns and five γ-turns.

The structure of the tetragonal form of *Af*PGA showed eight β-sheets and 27 helices. The α-chain consists of two strands and 11 helices, and the connecting part of the polypeptide chain forms one β-hairpin, two β-bulges and 11 β-turns. Similarly, the β-chain consists of 27 strands distributed in various β-sheets and 16 helices, and the connecting segment forms folds consisting of 12 β-hairpins, four β-bulges, 71 β-turns and six γ-turns. The domain architecture is the same in both crystal forms.

A binding site for a Ca^{2+} cation was located in the *Af*PGA structure. The calcium ion was identified as the highest peak present in the calculated difference Fourier map of both crystal forms and by comparison with the calcium-binding site in other PGAs. We could also find a major anomalous peak at the Ca position in a DANO map and a minor peak for a disulfide bond. Interestingly, we did not use calcium in the crystallization solution. We therefore believe that the bound metal atom must have come from the protein sample itself, based on a report of the presence of a tightly bound calcium ion in purified *Af*PGA (Kasche *et al.*, 2003). As previously mentioned, a bound calcium ion has also been reported at the same position in the *E. coli* and *P. rettgeri* PGA structures. Five of the six calcium-coordinating residues in *E. coli* PGA (Glu156, Asp336, Val338, Asp339 and Asp515; numbering according to the *E. coli* precursor enzyme) are conserved in *Af*PGA. The conserved calcium-binding residues in *Af*PGA are Gluα153, Aspβ73, Valβ75, Aspβ76 and Aspβ252 (Fig. 4*a*). In the case of the valine residue the coordination is through the main-chain carbonyl O atom, as is the case for Pro468 in *Ec*PGA, which is replaced by Ileβ205 in *Af*PGA.

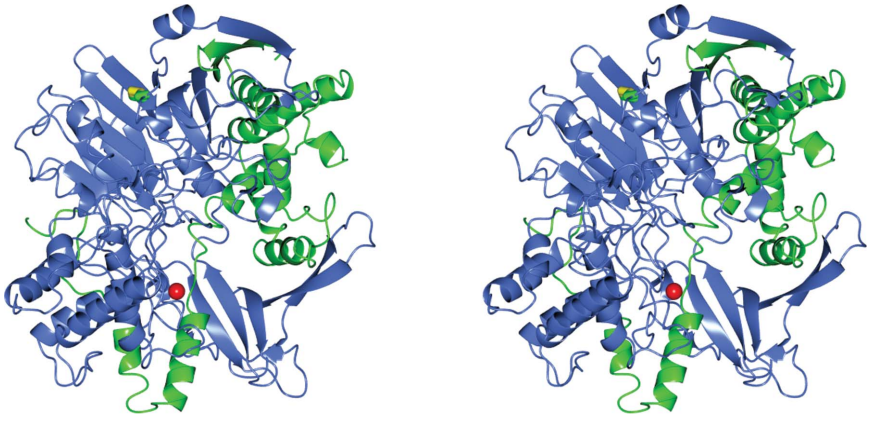

Figure 3
Stereoview of the three-dimensional structure of *Af*PGA showing the heterodimeric association (α-chains in green and β-chains in blue) and the $\alpha\beta\beta\alpha$ arrangement for the orthorhombic form (PDB entry 3k3w). The bound calcium ion is shown as a red ball and disulfide bonds are shown in yellow. This figure and Fig. 4 were prepared using *PyMOL* (DeLano, 2002).

4. Discussion

Penicillin acylases are important in the pharmaceutical industry for the production of semisynthetic β-lactam antibiotics *via* the key intermediate 6-aminopenicillanic acid. Pharmaceutical and biotechnological applications of penicillin acylases have emerged as a serious alternative to traditional chemical procedures for the manufacture of β-lactam antibiotics. Penicillin acylase-catalyzed processes are preferred in the industrial production of antibiotics owing to their environmental and economic benefits. The profound impact of penicillin acylases in pharmaceutical applications has sustained interest in identifying the structural determinants that are essential for catalysis by these enzymes. Efforts to enhance the catalytic rate by protein engineering have been reported (Alkema *et al.*, 2000, 2004; Alkema, Dijkhuis *et al.*, 2002; Alkema, Prins *et al.*, 2002; Gabor & Janssen, 2004; Jager *et al.*, 2007). In the cases of the PGAs from *E. coli* (Duggleby *et al.*, 1995) and *P. rettgeri* (McDonough *et al.*, 1999), the crystal structures of which are known, studies including substrate binding to selected site-directed mutants have allowed the mapping of some of the residues that constitute the active-site pocket of penicillin acylases (McVey *et al.*, 2001).

The PGA employed in semisynthetic penicillin manufacture is primarily sourced from *E. coli*. However, enzymes from other sources showing

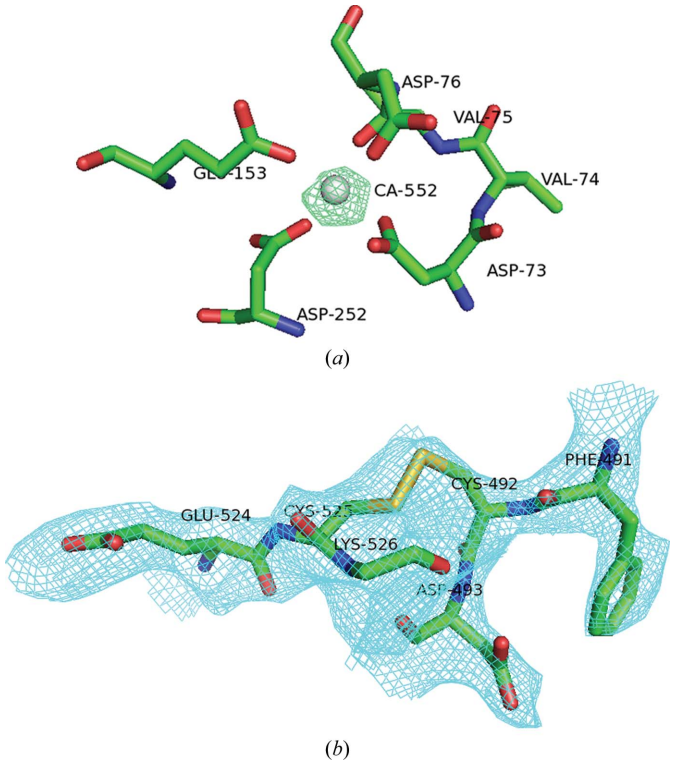

Figure 4
The calcium-binding site showing the residues (labelled as in *Af*PGA) involved in calcium binding. The electron density surrounding Ca is that of an $F_o - F_c$ map calculated in the absence of calcium and contoured at 6σ. (*b*) The disulfide bond (shown in yellow) formed by the two cystine residues β492 and β525 as observed in the orthorhombic form of *Af*PGA, together with the $2F_o - F_c$ electron-density map contoured at 1σ. Two neighbouring residues of each cystine are also shown. The same disulfide bond has also been identified in the tetragonal form (not shown).

higher thermostability and catalytic efficiency will be more attractive biocatalysts. The structure of the penicillin acylase from *A. faecalis* reported here is similar to the reported structures of the enzyme from other sources. The r.m.s. deviations for superposition of C^{α} atoms of the orthorhombic form (PDB entry 3k3w) on other structures are as follows: tetragonal form (PDB entry 3ml0), 0.71 Å; *Ec*PGA (PDB entry 1pnk; Duggleby *et al.*, 1995), 1.43 Å; Bro1 mutant *Pr*PGA (PDB entry 1cp9; McDonough *et al.*, 1999), 1.48 Å. The putative residues involved in catalysis (Serβ1, Gluβ23, Alaβ69 and Asnβ241) are conserved in all PGAs. We also identified a disulfide bridge in the *Af*PGA structure between cystine residues β492 and β525 which is absent in other penicillin acylases (Fig. 4*b*). This could be one of the factors that determine the higher thermostability of this enzyme. The structural similarity of *Af*PGA to other PGAs and its $\alpha\beta\beta\alpha$ architecture places it in the Ntn hydrolase superfamily and the free N-terminal residue Serβ1 has resulted from a post-translational autocatalytic proteolysis of the precursor enzyme, which has removed a linker peptide between the α- and β-chains. The three-dimensional structure reported here, although at moderate resolution, will help in carrying out a detailed analysis of all the factors that confer higher stability to this enzyme compared with other penicillin acylases. Information on stability factors will be useful when engineering penicillin acylases for industrial applications.

NKV and RSK thank the Council for Scientific and Industrial Research (CSIR), New Delhi for the award of research fellowships.

References

Alkema, W. B. L., Dijkhuis, A.-J., De Vries, E. & Janssen, D. B. (2002). *Eur. J. Biochem.* **269**, 2093–2100.
Alkema, W. B. L., Hensgens, C. M. H., Kroezinga, E. H., de Vries, E., Floris, R., van der Laan, J.-M., Dijkstra, B. W. & Janssen, D. B. (2000). *Protein Eng.* **13**, 857–863.
Alkema, W. B. L., Hensgens, C. M. H., Snijder, H. J., Keizer, E., Dijkstra, B. W. & Janssen, D. B. (2004). *Protein Eng. Des. Sel.* **17**, 473–480.
Alkema, W. B. L., Prins, A. K., de Vries, E. & Janssen, D. B. (2002). *Biochem. J.* **365**, 303–309.
Arroyo, M., de la Mata, I., Acebal, C. & Castillón, M. P. (2003). *Appl. Microbiol. Biotechnol.* **60**, 507–514.
Brannigan, J. A., Dodson, G., Duggleby, H. J., Moody, P. C., Smith, J. L., Tomchick, D. R. & Murzin, A. G. (1995). *Nature (London)*, **378**, 416–419.
Cowtan, K. (2006). *Acta Cryst.* D**62**, 1002–1011.
DeLano, W. L. (2002). *PyMOL*. http://www.pymol.org.
Deshpande, B. S., Ambedkar, S. S., Sudhakaran, V. K. & Shewale, J. G. (1994). *World J. Microbiol. Biotechnol.* **10**, 129–138.
Duggleby, H. J., Tolley, S. P., Hill, C. P., Dodson, E. J., Dodson, G. & Moody, P. C. (1995). *Nature (London)*, **373**, 264–268.
Emsley, P. & Cowtan, K. (2004). *Acta Cryst.* D**60**, 2126–2132.
Gabor, E. M. & Janssen, D. B. (2004). *Protein Eng. Des. Sel.* **17**, 571–579.
Guan, C., Cui, T., Rao, V., Liao, W., Benner, J., Lin, C.-L. & Comb, D. (1996). *J. Biol. Chem.* **271**, 1732–1737.
Ignatova, Z., Stoeva, S., Galunsky, B., Hörnle, C., Nurk, A., Piotraschke, E., Voelter, W. & Kasche, V. (1998). *Biotechnol. Lett.* **20**, 977–982.
Jager, S. A. W., Jekel, P. A. & Janssen, D. B. (2007). *Enzyme Microb. Technol.* **40**, 1335–1344.
Kasche, V., Galunsky, B. & Ignatova, Z. (2003). *Eur. J. Biochem.* **270**, 4721–4728.
Kasche, V., Lummer, K., Nurk, A., Piotraschke, E., Rieks, A., Stoeva, S. & Voelter, W. (1999). *Biochim. Biophys. Acta*, **1433**, 76–86.
Laskowski, R. A., MacArthur, M. W., Moss, D. S. & Thornton, J. M. (1993). *J. Appl. Cryst.* **26**, 283–291.
Lee, J. J., Ekker, S. C., von Kessler, D. P., Porter, J. A., Sun, B. I. & Beachy, P. A. (1994). *Science*, **266**, 1528–1537.
Lowry, O. H., Rosebrough, N. J., Farr, A. L. & Randall, R. J. (1951). *J. Biol. Chem.* **193**, 265–275.
Matthews, B. W. (1968). *J. Mol. Biol.* **33**, 491–497.
McCoy, A. J., Grosse-Kunstleve, R. W., Adams, P. D., Winn, M. D., Storoni, L. C. & Read, R. J. (2007). *J. Appl. Cryst.* **40**, 658–674.
McDonough, M. A., Klei, H. E. & Kelly, J. A. (1999). *Protein Sci.* **8**, 1971–1981.
McVey, C. E., Walsh, M. A., Dodson, G. G., Wilson, K. S. & Brannigan, J. A. (2001). *J. Mol. Biol.* **313**, 139–150.
Murshudov, G. N., Skubák, P., Lebedev, A. A., Pannu, N. S., Steiner, R. A., Nicholls, R. A., Winn, M. D., Long, F. & Vagin, A. A. (2011). *Acta Cryst.* D**67**, 355–367.
Oinonen, C. & Rouvinen, J. (2000). *Protein Sci.* **9**, 2329–2337.
Otwinowski, Z. & Minor, W. (1997). *Methods Enzymol.* **276**, 307–326.
Parmar, A., Kumar, H., Marwaha, S. S. & Kennedy, J. F. (2000). *Biotechnol. Adv.* **18**, 289–301.
Petrovan, R. J., Govers-Riemslag, J. W. P., Nowak, G., Hemker, H. C., Tans, G. & Rosing, J. (1998). *Biochemistry*, **37**, 1185–1191.
Sizmann, D., Keilmann, C. & Böck, A. (1990). *Eur. J. Biochem.* **192**, 143–151.
Stennicke, H. R. & Salvesen, G. S. (1998). *Biochim. Biophys. Acta*, **1387**, 17–31.
Suresh, C. G., Pundle, A. V., SivaRaman, H., Rao, K. N., Brannigan, J. A., McVey, C. E., Verma, C. S., Dauter, Z., Dodson, E. J. & Dodson, G. G. (1999). *Nature Struct. Biol.* **6**, 414–416.
Verhaert, R. M., Riemens, A. M., van der Laan, J.-M., van Duin, J. & Quax, W. J. (1997). *Appl. Environ. Microbiol.* **63**, 3412–3418.
Wang, Y. & Guo, H.-C. (2010). *J. Mol. Biol.* **403**, 120–130.
Winn, M. D. *et al.* (2011). *Acta Cryst.* D**67**, 235–242.
Wu, Z., Yao, N., Le, H. V. & Weber, P. C. (1998). *Trends Biochem. Sci.* **23**, 92–94.
Zlotnick, A., Reddy, V. S., Dasgupta, R., Schneemann, A., Ray, W. J., Rueckert, R. R. & Johnson, J. E. (1994). *J. Biol. Chem.* **269**, 13680–13684.